Article

Gut microbe-generated phenylacetylglutamine is an endogenous allosteric modulator of β2-adrenergic receptors

Prasenjit Prasad Saha[1,2], Valentin Gogonea[1,2,3], Wendy Sweet[1], Maradumane L. Mohan [1], Khuraijam Dhanachandra Singh[1], James T. Anderson [1,2], Deepthi Mallela [1,2], Conner Witherow[1], Niladri Kar [1], Kate Stenson[1], Terri Harford [1], Michael A. Fischbach [4], J. Mark Brown [1,2], Sadashiva S. Karnik [1], Christine S. Moravec[1], Joseph A. DiDonato [1,2], Sathyamangla Venkata Naga Prasad[1] & Stanley L. Hazen [1,2,5] ✉

Allosteric modulation is a central mechanism for metabolic regulation but has yet to be described for a gut microbiota-host interaction. Phenylacetylglutamine (PAGln), a gut microbiota-derived metabolite, has previously been clinically associated with and mechanistically linked to cardiovascular disease (CVD) and heart failure (HF). Here, using cells expressing β1- versus β2-adrenergic receptors (β1AR and β2AR), PAGln is shown to act as a negative allosteric modulator (NAM) of β2AR, but not β1AR. In functional studies, PAGln is further shown to promote NAM effects in both isolated male mouse cardiomyocytes and failing human heart left ventricle muscle (contracting trabeculae). Finally, using in silico docking studies coupled with site-directed mutagenesis and functional analyses, we identified sites on β2AR (residues E122 and V206) that when mutated still confer responsiveness to canonical β2AR agonists but no longer show PAGln-elicited NAM activity. The present studies reveal the gut microbiota-obligate metabolite PAGln as an endogenous NAM of a host GPCR.

In recent years, significant interest has been directed toward the role of gut microbiome-host interactions in human health, particularly in cases where gut microbiota-derived metabolites may contribute directly to disease susceptibility[1–7]. Phenylacetylglutamine (PAGln) is a recently discovered CVD-linked gut microbial metabolite that is associated with incident risk for major adverse cardiovascular events (MACE, myocardial infarction (MI), stroke, or death)[8], and both clinically and mechanistically linked to both the presence and severity of heart failure (HF)[9,10]. Circulating levels of PAGln have also recently been reported to be associated with both coronary athero-sclerotic burden among patients with suspected coronary artery disease[11] and in-stent stenosis and hyperplasia in subjects with coronary artery disease[12]. The gut microbiota-dependent production of PAGln from dietary phenylalanine involves two distinct microbial pathways—one catalyzed by phenylpyruvate:ferredoxin oxidor-eductase (PPFOR) and the other by phenylpyruvate decarboxylase

[1]Department of Cardiovascular & Metabolic Sciences, Lerner Research Institute, Cleveland Clinic, 9500 Euclid Ave., Cleveland, OH, USA. [2]Center for Microbiome & Human Health, Cleveland Clinic, 9500 Euclid Ave., Cleveland, OH, USA. [3]Chemistry Department, Cleveland State University, 2121 Euclid Ave., Cleveland, OH, USA. [4]Department of Bioengineering and ChEM-H, Stanford University, Stanford, CA, USA. [5]Heart, Vascular and Thoracic Institute, Cleveland Clinic, Cleveland, OH, USA. ✉e-mail: hazens@ccf.org

(PPDC)[13]. Like circulating levels of PAGln itself, the fecal levels of both PPFOR and PPDC are associated with atherosclerotic cardiovascular disease[13]. Beyond clinical association studies, mechanistic studies indicate a link between PAGln and CVD pathogenesis. For example, PAGln has been shown to enhance platelet responsiveness in studies with isolated human platelets, and to promote in vivo thrombosis potential in animal models of CVD, exerting its effects at least in part via platelet G-protein coupled receptors (GPCRs)[8]. These were shown to include α2A, α2B, and β2-adrenergic receptors (β2AR)[8], which play a crucial role in regulating cardiac function and maintaining cardiometabolic homeostasis[14–16]. PAGln is the first reported gut microbe-derived metabolite to mediate cellular responses through adrenergic receptors (ARs). However, the precise mechanism by which PAGln modulates ARs is unknown.

Allosteric modulation is a central mechanism for the "fine-tune" regulation of biological pathways and/or processes. This is achieved by modulating the binding affinity of ligands to their respective receptors, by modulating the signaling efficacy of ligands to their respective receptor, or by a combination of both mechanisms. Despite the recognition that microbial symbionts have evolved with their hosts and can produce bioactive metabolites that impact host pathophysiological processes, demonstration of microbe-host interactions via an allosteric modulator of host receptor signaling or enzyme catalysis has not yet been reported.

Adrenergic receptors (ARs) play a critical role in many metabolic, cardiovascular and homeostatic functions, and are particularly numerous in the heart, vasculature, neurons, and adipose tissue[17,18]. Members of the G protein coupled receptor (GPCR) superfamily, the 9 ARs are further sub-divided into two major groups: α- and β-adrenoceptors. βARs play a central role in the overall regulation of cardiac function, whereas αARs play an important role in the regulation of blood pressure[19,20]. Given their pharmacological potential, there has been growing interest in developing synthetic compounds that can bind to GPCRs like ARs at sites topologically distinct from the orthosteric binding site where the endogenous canonical ligands norepinephrine and epinephrine interact (i.e., to function as an allosteric ligand). In fact, several synthetic compounds have been developed that bind at allosteric (non-orthosteric) sites, enabling fine-tuning of the GPCRs' functional output[21–24]. For example, recent studies on β2AR have identified several synthetic ligands that act as either a positive allosteric modulator (PAM), or a negative allosteric modulator (NAM) for β2AR, and crystallography studies with these agents have revealed allosteric binding pockets distinct from the orthosteric site[25–29]. Within the context of nine adrenergic receptors, this manuscript centers on exploring the interaction between PAGln and both β1 and β2ARs as model receptors. This emphasis is guided by the robust clinical associations of circulating PAGln levels with phenotypes pertinent to heart failure[9,10,30], and the known clinical links between βARs and heart failure[31,32].

While synthetic allosteric modulators have been documented for β2AR, there is currently no evidence, to the best of our knowledge, supporting the existence of endogenous allosteric modulators affecting adrenergic receptors. Similarly, no reported instances are known, to our knowledge, of a gut microbiome-generated metabolite acting as an allosteric modulator for a host receptor. Here, we provide multiple lines of evidence demonstrating that the gut microbe-generated metabolite PAGln functions as an endogenous NAM of β2AR. Further, we identify a conformational hub involving at least two receptor residues—distant by primary sequence but in close spatial proximity based on the β2AR crystal structure—that are critical for propagation of PAGln-mediated NAM activity. Finally, our studies show that PAGln NAM activity supports an overall negative inotropic functional effect in cardiomyocytes and within the failing human heart under conditions of sympathetic tone.

Results

Acute exposure to PAGln in the absence of canonical AR ligand fosters transient weak agonist effect with β2AR, but not β1AR

Since PAGln was recently shown to mediate cellular events via adrenergic receptors (ARs)[8], and given its strong clinical associations with heart failure[9], we sought to decipher underlying receptor-ligand interaction events mediated by PAGln using β1AR and β2AR as model receptors. To test whether PAGln directly regulates the function of β1AR and/or β2AR, we initially applied varying doses of PAGln to parental-HEK293 cells, which possess low background AR levels (~34 fmol/mg protein) versus either β1-HEK293 or β2-HEK293 cells stably over-expressing their respective ARs[8]. We then monitored resulting cAMP production as illustrated in the experimental scheme shown in Fig. S1A. For all studies, levels of PAGln used were well within the range observed under physiological conditions. For example, in an angiographic cohort of subjects with predominantly preserved renal function[8], PAGln levels of 10 μM, 100 μM, and 267 μM corresponded to the 95%ile, 99%ile, and maximum fasting plasma levels noted, respectively. In subjects with renal dysfunction, such as chronic kidney disease and end stage renal disease, substantially higher levels of PAGln have been reported[33–35]. Notably, PAGln by itself (100 μM) failed to induce cAMP production in β1-HEK293 cells, like the precursor amino acid of PAGln, phenylalanine (Phe), which was used as a negative control. In contrast, in the β2-HEK293 cells, PAGln dose-dependently induced a transient (only with acute exposures <10 min) and sub-optimal cAMP generation (EC_{50} of 23 ± 3.5 μM), consistent with the properties of a partial agonist (Fig. 1A, B; Fig. S1B). In contrast to the weak and transient response with PAGln, robust cAMP dose-responses were observed when the known agonists of βAR isoproterenol (ISO) and norepinephrine (NE) were used as positive controls (EC_{50}s of 0.5 ± 0.05 nM and 9.4 ± 1.2 nM, respectively, with β2-HEK293 cells; and 7.7 ± 0.7 nM and 22.6 ± 2.7 nM, respectively, with β1-HEK293 cells; Fig. 1A, B).

PAGln primarily functions as a NAM of β2AR but not β1AR: cAMP production and β-arrestin2 recruitment

We next examined the effect of PAGln on β1AR or β2AR under more physiologically relevant conditions where PAGln co-exists with β-agonists. For these studies, cells were exposed to PAGln chronically before addition of canonical AR ligands. Results with ≥15 min exposures to PAGln, followed by 10 min β-agonist incubation, showed similar results; thus, all studies thereafter were performed as indicated in the Scheme shown in Fig. S1C as detailed in Methods. For these studies, full dose-response functional assays (cAMP induction) for the canonical AR ligands ISO and NE were examined in the presence versus absence of physiological levels of PAGln for both β1AR and β2AR (i.e., in both β1-HEK293 and β2-HEK293 cells). Notably, when pre-incubated with PAGln, ISO-treated β2-HEK293 cells showed a significant ($P < 0.0001$; ISO EC_{50}: 0.6 ± 0.1 nM vs ISO+PAGln EC_{50}: 3.2 ± 0.4 nM) rightward shift (5.3 ± 0.8-fold higher EC_{50} in the presence of PAGln; $P = 0.04$) of the ISO-induced cAMP dose-response curve, indicating that PAGln functions as an α- (change in affinity) negative allosteric modulator (α-NAM) of β2AR (Fig. 1C). By contrast, in β1-HEK293 cells, co-incubation with PAGln failed to shift the dose-response curve of ISO-induced cAMP production ($P = 0.75$, Fig. 1D). In parallel studies using NE instead of ISO as βAR agonist, the presence of PAGln similarly induced a significant rightward shift ($P < 0.0001$; NE EC_{50}: 7.3 ± 1.4 nM vs NE+PAGln EC_{50}: 31 ± 3.4 nM) of the NE-induced cAMP production dose-response curve (4.2 ± 1.7-fold higher EC_{50}; $P = 0.04$) in β2-HEK293 cells (Fig. 1E). In contrast, PAGln again failed to show any NAM activity in β1-HEK293 cells with the alternative βAR agonist NE ($P = 0.47$, Fig. 1F). We also monitored the effect of PAGln dose response on cAMP production when using fixed EC_{50} doses of ISO (EC_{50} 0.5 nM) or NE (EC_{50} 22.6 nM). Across the pathophysiologically relevant and lower range of concentrations (10–300 μM), PAGln dose-dependently
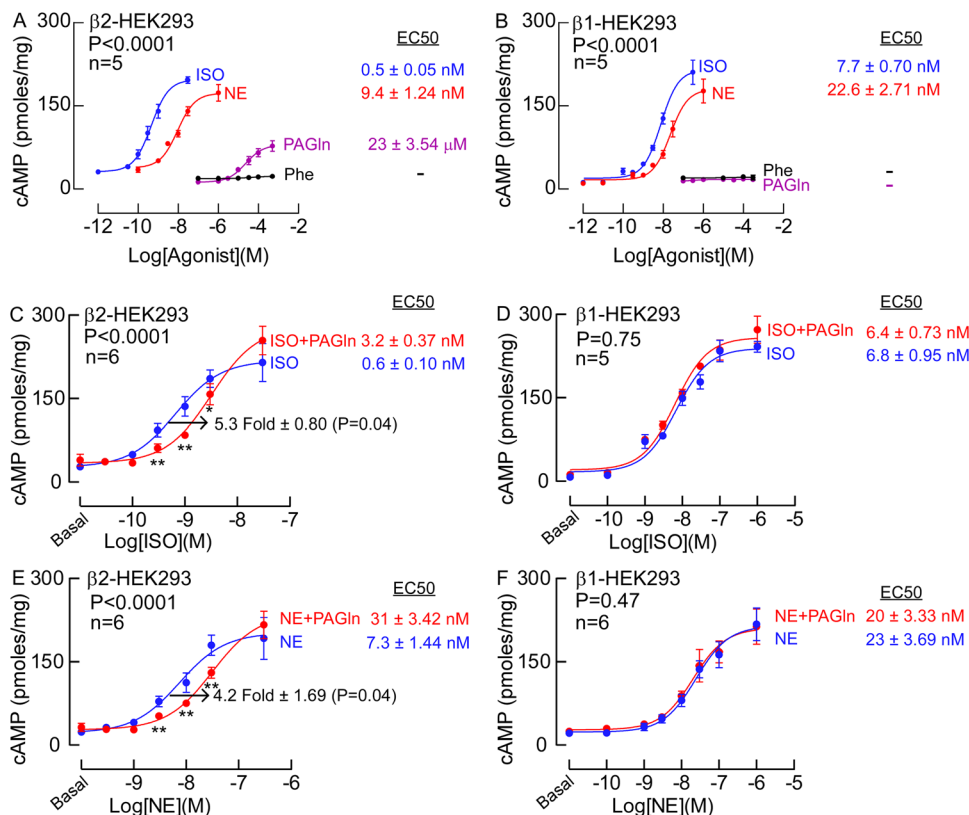
Fig. 1 | cAMP dose-responses with different agonists in HEK293 cells.
A Intracellular cAMP production in stably transfected β2-HEK293 cells after treating them with increasing concentration of isoproterenol (ISO) (Blue), norepinephrine (NE) (Red), phenylacetylglutamine (PAGln) (Purple) and phenylalanine (Phe) (Black) as indicated. **B** Intracellular cAMP production in stably transfected β1-HEK293 cells after treating them with increasing concentration of isoproterenol (ISO) (Blue), norepinephrine (NE) (Red), phenylacetylglutamine (PAGln) (Purple) and phenylalanine (Phe) (Black) as indicated. ISO and NE serve as positive controls and phenylalanine (Phe) serves as negative control. **C** cAMP dose-response in stably transfected β2-HEK293 cells after treating the cells with isoproterenol (ISO) alone (Blue), or ISO along with 100 μM PAGln (Red), pre-incubated for 15 min ($P < 0.0001$; EC_{50} Blue vs Red). For ISO-induced cAMP dose-response, PAGln pre-incubation in β2-HEK293 displayed 5.3 ± 0.80-fold increase ($P = 0.04$) in the EC_{50} as compared to the ISO alone control. Two-tailed unpaired Welch's student t-test was used to obtain the fold change P-value by comparing the mean EC_{50} values of ISO and ISO +PAGln from three different experiments (ISO vs ISO+PAGln; $P = 0.04$). **D** cAMP dose-response in stably transfected β1-HEK293 cells after treating the cells with isoproterenol (ISO) alone (Blue), or ISO along with 100 μM PAGln (Red), pre-

incubated for 15 min ($P = 0.75$; EC_{50} Blue vs Red). **E** cAMP dose-response curves of norepinephrine (NE) alone (Blue) and NE along with 100 μM PAGln (Red), pre-incubated for 15 min in stably transfected β2-HEK293 cells ($P < 0.0001$; EC_{50} Blue vs Red). PAGln pre-incubation in β2-HEK293 displays 4.2 ± 1.69-fold increase ($P = 0.04$) in the EC_{50} of the dose-response of NE pre-incubated with PAGln as compared to NE alone control. Two-tailed unpaired Welch's student t-test was used to obtain the fold change P-value when comparing the EC_{50} values for NE and NE+PAGln from three different experiments (NEvs NE+PAGln; $P = 0.04$). **F** cAMP dose-response curves of norepinephrine (NE) alone (Blue) and NE along with 100 μM PAGln (Red), pre-incubated for 15 min in stably transfected β1-HEK293 cells ($P = 0.47$; EC_{50} Blue vs Red). Data points represent the mean ± SD of the indicated number (n) of experiments. P values (top left) for EC_{50} comparisons (Blue vs Red) as well as the standard error of the mean EC_{50} (SEM) were determined with a non-linear regression method and the significance of the fold changes was analyzed using two-tailed unpaired Welch's student t-test. Nonparametric two-tailed Mann–Whitney test was used for non-pairwise comparisons (*$P \le 0.05$; **$P \le 0.01$; ***$P \le 0.001$). All reported P values are two-sided. A P-value of <0.05 was considered significant in this study.

reduced both ISO- and NE-induced cAMP production in β2-HEK293 cells, further validating its function as a NAM (Fig. S1D and S1E). The ability of PAGln to elicit NAM effects in β2AR-expressing HEK293 cells, but not in β1AR-expressing HEK293 cells, was further verified in multiple independent experiments (Fig. 1 and Fig. S1).

In further studies we examined whether PAGln could modulate β-arrestin2 recruitment using the PRESTO-Tango reporter system[36]. Using this model reporter system in β2-expressing cells, physiological levels of PAGln elicited β-NAM (change in efficacy) properties when concomitantly incubated with βAR agonists (either ISO or NE), demonstrating a significant reduction in agonist-induced maximal β-arrestin2 recruitment (β-NAM activity), both with ISO (Fig. 2A) (ISO B_{max}: 3361 RLU vs ISO+PAGln B_{max}: 2469 RLU; $P < 0.0001$) and NE (Fig. 2C) (NE B_{max}: 3137 RLU vs NE+PAGln B_{max}: 2163 RLU; $P < 0.0001$) (Fig. 2A, C). We again observed specificity of PAGln-induced NAM activity for β2AR, but not β1AR, as PAGln failed to show any significant effect when monitoring either ISO- or NE-induced β-arrestin2 recruitment in β1-HTLA cells ($P > 0.05$ for all comparisons, Fig. 2B, D). Similar

to the results of the cAMP studies, concentrations of PAGln across physiological levels (e.g., as low as 3 μM) were observed to significantly reduce both ISO- and NE-induced β-arrestin2 recruitment in β2AR expressing β2-HTLA cells (Figs. S2A and S2B) when fixed concentration of ISO (EC_{50} 47 nM) and NE (EC_{50} 17 μM) were used. Importantly, incubation with PAGln alone had no effect on β2AR-dependent β-arrestin2 recruitment, consistent with PAGln functioning as an allosteric modulator (Fig. S2).

Competition and saturation binding studies further confirm that PAGln functions as a NAM of β2AR

To confirm the ability of PAGln to function as a NAM for β2AR, we next examined whether an excess of PAGln can markedly suppress the direct binding of an orthosteric ligand to β2AR. Accordingly, we examined interaction of the orthosteric ligand [^{3}H]-propranolol with β2AR by pre-incubating β2-HEK293 cell membranes with PAGln. PAGln alone, even in large molar excess (1 mM), failed to inhibit [^{3}H]-propranolol binding to β2AR, confirming that PAGln binds at a site on
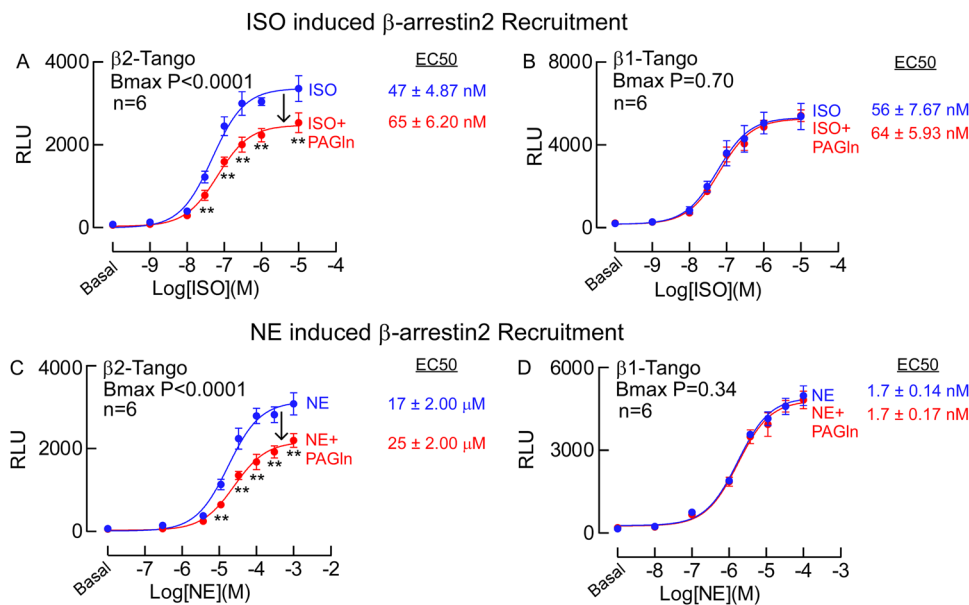
Fig. 2 | Effect of PAGln pre-incubation on ISO- and NE-induced β-arrestin2 recruitment to β2AR in HTLA cells. A β-arrestin2 recruitment induced by increasing concentration of isoproterenol (ISO) alone (Blue) or ISO along with 100 μM PAGln (Red), in β2-Tango transfected cells ($P < 0.0001$; B_{max} Blue vs Red). **B** β-arrestin2 recruitment induced by increasing concentration of isoproterenol (ISO) alone (Blue) or ISO along with 100 μM PAGln (Red), in β1-Tango transfected cells ($P = 0.7$; B_{max} Blue vs Red). **C** Norepinephrine (NE) alone (Blue) and NE along with 100 μM PAGln (Orange) induced dose-response of β-arrestin2 recruitment in β2-Tango transfected cells ($P < 0.0001$; B_{max} Blue vs Red). **D** Norepinephrine (NE) alone (Blue) and NE along with 100 μM PAGln (Red) induced dose-response of β-arrestin2 recruitment in β1-Tango transfected cells ($P = 0.3$; B_{max} Blue vs Red). β-arrestin2 recruitment was measured as relative luminance unit (RLU). Data points represent the mean ± SD of the indicated number (n) of experiments. P values (top left) for B_{max} comparisons (Blue vs Red) as well as the EC_{50}s and the standard error of the mean EC_{50} (SEM) were determined with a non-linear regression method. Nonparametric two-tailed Mann–Whitney test was used for non-pairwise comparisons (*$P \le 0.05$; **$P \le 0.01$; ***$P \le 0.001$). All reported P values are two-sided. A P-value of <0.05 was considered significant in this study.

β2AR distinct from the binding site of [3H]-propranolol (i.e., the orthosteric site) (Fig. 3A, black line). However, the presence of PAGln diminished the ability of non-labeled ISO ($P < 0.0001$; ISO EC_{50}: 1.8 ± 0.14 μM vs ISO+PAGln EC_{50}: 4.4 ± 0.31 μM) to compete for [3H]-propranolol binding to β2AR (i.e., in the presence of PAGln there was a 2.4 ± 0.07-fold increase in the observed EC_{50} of ISO binding competition to [3H]-propranolol; Fig. 3A; $P = 0.001$), thereby demonstrating that PAGln can elicit α-NAM activity on β2AR binding to an orthosteric agonist (ISO).

Previous studies using the synthetic β2AR NAM AS408 show that it can also function as a modest PAM for antagonist/inverse agonist binding[27], so we next explored whether PAGln may function similarly. β2-HEK293 cell membranes (and control parental cell membranes) were incubated with increasing concentrations of the β2-antagonist [3H]-propranolol, either with or without PAGln. When β2-HEK293 cell membranes were pre-incubated with PAGln, a modest but significant enhancement (2.1 ± 0.3-fold reduction in K_d; $P = 0.01$) in saturable and specific binding of [3H]-propranolol to β2AR was observed (K_d: [3H]-propranolol alone, 0.77 ± 0.15 nM, [3H]-propranolol + PAGln, 0.36 ± 0.07 nM) (Fig. 3B). In contrast, pre-incubation of the β2-HEK293 cell membranes with an excess (10 mM) of ISO blocked a majority of [3H]-propranolol specific, saturable binding, and only nonspecific binding was observed (Fig. 3B). We observed a similar modest increase (in the presence of PAGln) in the binding of the antagonist [3H]-dihydroalprenolol ([3H]-DHAP) to β2-HEK293 cell membranes ($P < 0.0007$; [3H]-DHAP K_d: 0.8 ± 0.12 nM vs [3H]-DHAP+PAGln K_d: 4.2 ± 0.08 nM and 1.9 ± 0.39-fold reduction in K_d; $P = 0.04$) (Fig. S3A). PAGln also modestly enhanced the affinity of the inverse agonist ICI118,551 for β2AR in binding competition to [3H]-propranolol ($P < 0.04$; ICI118,551 IC_{50}: 0.8 ± 0.12 nM vs ICI118,551 +PAGln IC_{50}: 4.2 ± 0.08 nM and reduction in IC_{50} of approximately 1.4 ± 0.16-fold; $P = 0.1$) (Fig. S3B). Similarly, for [3H]-DHAP, we observed a modest enhanced affinity of ICI118,551 binding, although not statistically significant ($P < 0.18$; ICI118,551 IC_{50}:

0.92 ± 0.19 nM vs ICI118,551 +PAGln IC_{50}: 0.67 ± 0.09 nM and reduction in EC_{50} of -1.4 ± 0.46-fold; $P = 0.37$) (Fig. S3C).

In complementary studies, we examined the NAM properties of PAGln in the presence of the agonist ISO using the label-free assay technology dynamic mass redistribution (DMR), which enables real-time detection of receptor ligand-dependent integrated cellular responses in live cells[8,37]. Pre-incubation of β2-HEK293 cells with PAGln reliably induced a significant decrease in the ISO-induced maximum DMR response at different ISO concentration examined (ISO concentration from 1 nM to 100 nM; $P < 0.05$), consistent with PAGln promoting a β-NAM effect on ISO binding to β2AR ($P < 0.0001$; B_{max} ISO vs ISO+PAGln) (Fig. 3C).

PAGln induces a negative inotropic effect in failing human ventricular tissue

Having determined that PAGln functions as a NAM of β2AR in both cell culture models and in isolated β2AR expressing cell membranes, we next examined whether PAGln affects human heart function via NAM action. While β1AR predominates over β2AR in human ventricular tissue, the content of β2AR increases in heart failure[38–40]. Consequently, we aimed to investigate whether PAGln elicits negative allosteric effects in functional assays conducted on left ventricular trabecular muscles derived from failing human hearts. Failing human heart tissue was recovered at the time of open-heart surgery ("Methods"), and isometric muscle contraction was measured in isolated left ventricular (LV) trabecular muscle in response to the endogenous β-agonist NE, either with or without PAGln (Fig. 4). In the presence of PAGln ($n = 9$ subjects, $n = 14$ LV samples), the dose-response curve for NE-induced LV muscle contraction was significantly shifted to the right compared to samples exposed only to NE ($n = 6$ subjects, $n = 11$ LV samples), indicating a significant NAM effect ($P = 0.002$; NE EC_{50}: 0.24 ± 0.06 μM vs NE +PAGln EC_{50}: 0.6 ± 0.13 μM), with an increased EC_{50} of $\sim 2.5 \pm 0.29$-

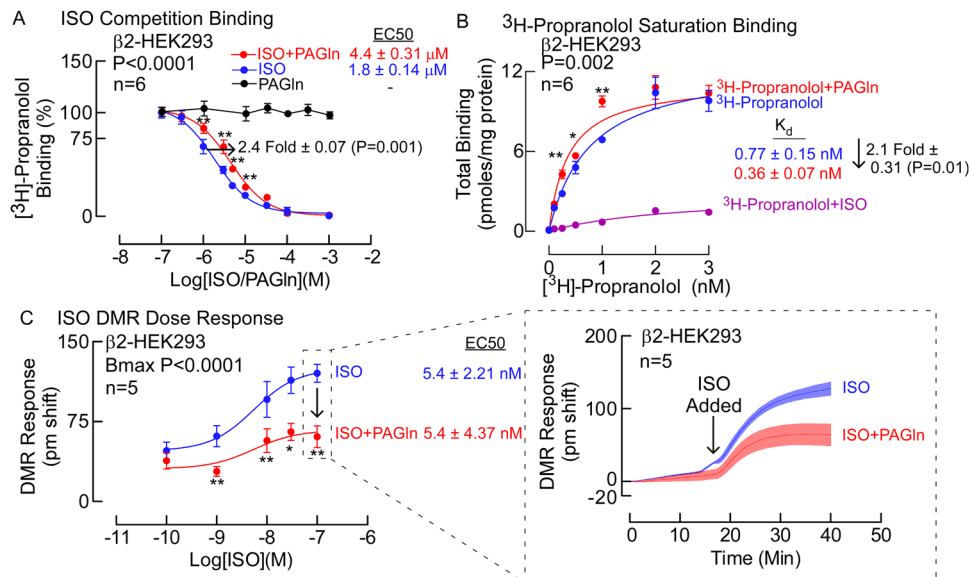**Fig. 3 | PAGln effect on binding of orthosteric ligand [³H]-propranolol and ISO-induced dynamic mass redistribution (DMR) on β2AR. A** Competition binding dose-response curve of PAGln alone (Black), isoproterenol (ISO) alone (Blue), or ISO with 100 μM PAGln (Red) to the β2-HEK293 cell membranes with [³H]-propranolol ($P < 0.0001$; EC_{50} Blue vs Red). PAGln pre-incubation in β2-HEK293 displays 2.4 ± 0.07-fold increase ($P = 0.001$) in the EC_{50} of the dose-response as compared to ISO alone control. Two-tailed unpaired Welch's student t-test was used to obtain the fold change P-value when comparing the EC_{50} values for ISO and ISO+PAGln from three different experiments (ISO vs ISO+PAGln; $P = 0.001$). **B** Saturation-binding in β2-HEK293 cell membranes with increasing concentrations of orthosteric ligand [³H]-propranolol alone (Blue), [³H]-propranolol along with 100 μM PAGln (Red) or 10 mM ISO (Purple) ($P = 0.002$; K_d Blue vs Re$_d$). PAGln pre-incubation in β2-HEK293 displays 2.1 ± 0.3-fold decrease ($P = 0.01$) in the K_d as compared to ISO alone control. Two-tailed unpaired Welch's student t-test was used to obtain the fold change P-value when comparing the K_d values for [³H]-

propranolol and [³H]-propranolol +PAGln from three different experiments ([³H]-propranolol vs [³H]-propranolol +PAGln; $P = 0.01$). **C** ISO-induced dynamic mass redistribution (DMR) dose-response in β2-HEK293 cells alone (Blue) and in presence of 100 μM PAGln (Red). DMR response of 0.1 μM ISO and 0.1 μM ISO along with 100 μM PAGln are highlighted in the dashed box right side. EC_{50} of ISO and ISO +PAGln are indicated ($P = 0.98$; EC_{50} Blue vs Red). Data points represent the mean ± SEM (for PAGln alone; Fig. 3A) and mean ± SD (for the rest) of the indicated number (n) of experiments. P values (top left) for EC_{50} comparisons (Blue vs Red) as well as the standard error of the mean EC_{50} (SEM) were determined with a non-linear regression method and the significance of the fold changes was analyzed using two-tailed unpaired Welch's student t-test. Nonparametric two-tailed Mann–Whitney test was used for non-pairwise comparisons (*$P \leq 0.05$; **$P \leq 0.01$; ***$P \leq 0.001$). All reported P values are two-sided. A P-value of <0.05 was considered significant in this study.

fold ($P = 0.01$) (Fig. 4). This reduced degree of NE-induced LV contraction in the presence of PAGln is consistent with its function as an α-NAM in human LV tissue. The data also show that PAGln induces a negative inotropic effect in failing human ventricular tissue.

PAGln induces a negative inotropic effect on isolated murine cardiomyocytes

To further demonstrate that PAGln can directly function as a negative allosteric modulator under physiological conditions, we also examined an ISO-induced murine model of ventricular cardiomyocyte contraction (Fig. 5). We observed no effect on cardiomyocyte contraction (as monitored by sarcomere shortening/length) when electrically paced freshly-isolated ventricular cardiomyocytes were incubated with PAGln alone (or vehicle). In contrast, when cardiomyocytes were treated with ISO, we observed a significant enhancement in sarcomere shortening compared to vehicle or PAGln alone. Notably, pre-incubation with PAGln significantly reduced the extent of ISO-induced cardiomyocyte contraction, consistent with functioning as an NAM, and overall eliciting a negative inotropic effect (i.e., the reduction in sarcomere shortening is only observed in the presence of the canonical AR ligand; Fig. 5C, D). A similar negative inotropic effect, only in the concomitant presence of the βAR agonist ISO, was observed using phenylacetylglycine (PAGly) (Fig. 5E, F), the gut microbe-generated counterpart to PAGln observed at higher abundance in mice[8]. Together, these results are consistent with PAGln (and PAGly) acting as an endogenous NAM of β2AR function during human and mouse heart muscle contraction.

Identifying β2AR residues that contribute to PAGln-mediated NAM activity

We next sought to identify key amino acid residues of β2AR involved in either PAGln binding and/or propagation of its NAM signaling. For these studies we used multiple different approaches to identify candidate residues in β2AR for site-directed mutagenesis, ranging from In silico docking studies to targeting of residues within previously reported binding pockets for synthetic allosteric modulators of β2AR revealed by crystallography studies. Details of residue selection for mutagenesis, and both methods and results of functional interrogations are outlined within Supplemental Methods (Tables S1–S5, Figs. S4–S15). In brief, recombinant β2AR mutants were assayed for both functional activity with canonical ligands (to ensure the mutant receptors still functioned), and for PAGln-elicited NAM activity (to explore the effect of site-specific mutation on PAGln-driven allosteric effect). Figure 6 shows four overlapping β2AR structures[26–28], along with the canonical endogenous ligand isoproterenol bound to the orthosteric site, and PAGln docked to each of 5 candidate binding sites on β2AR: two candidate binding sites in the extracellular domain (what we termed ECDbs₂ and ECDbs₅) or each of the three distinct previously reported allosteric sites (allosteric sites 1, 2, and 3 which we termed; AS1, AS2 and AS3), where the synthetic NAM AS408, synthetic PAM Cmpd-6FA, and synthetic NAM Cmpd-15PA, respectively, co-crystalized with β2AR[26–28]. Notably, of all the differing amino acid residues of β2AR tested for involvement in PAGln-dependent propagation of NAM signaling (Tables S1–S5, Figs. S4–S15), only site-directed mutagenesis of residues previously identified in the binding pocket of a synthetic NAM, AS408, were found to participate in PAGln-mediated
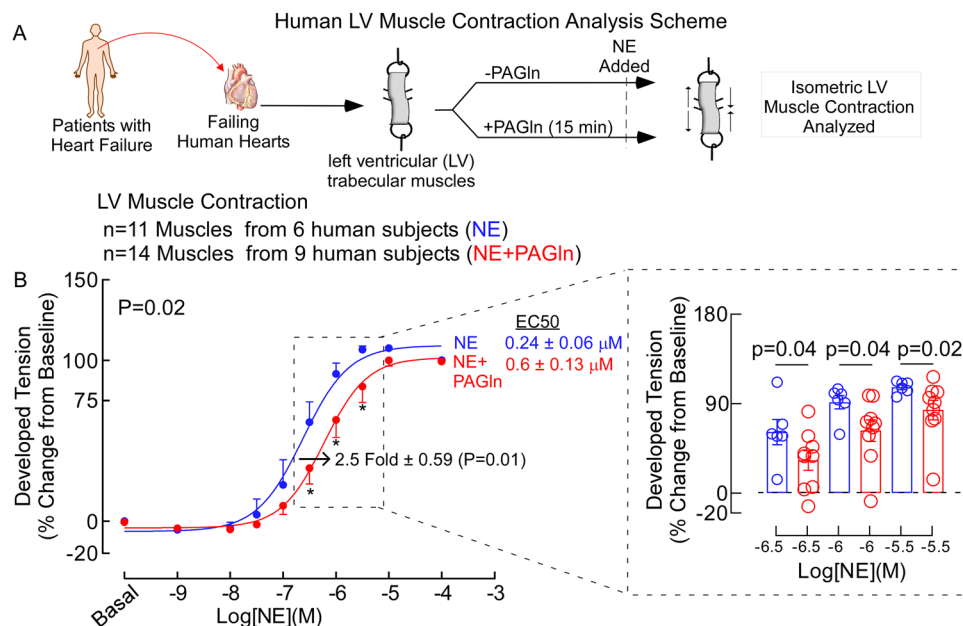
Fig. 4 | NE-induced human LV muscle contraction in presence or in absence of PAGln. A, B Flowchart describing the isometric human left ventricular (LV) muscle contraction analysis scheme. **A** LV trabecular tissue was removed from patients with heart failure and isometric muscle contraction was measured treating the tissues with increasing concentration of norepinephrine (NE) alone (Blue) and in presence of 100 μM PAGln (Red) ($P = 0.02$; EC_{50} Blue vs Red), exhibiting 2.5 ± 0.59-fold ($P = 0.01$) increased EC_{50} following PAGln incubation. **B** Individual data points (mean value of each heart subject) from selected concentrations are highlighted in the dashed box (right). PAGln pre-incubation displays 2.5 ± 0.59-fold increase in the EC_{50} of the dose-response as compared to NE alone control ($P = 0.01$). Two-tailed unpaired Welch's student t-test was used to obtain the fold change P-value when comparing the EC_{50} values of NE and NE + PAGln calculated for individual human subject muscles (NE+PAGln; $P = 0.01$). Data points represent the mean ± SD (n = number of heart muscles). P value (top left) for EC_{50} comparison (Blue vs Red) was determined with a non-linear regression method. Nonparametric two-tailed Mann–Whitney test was used for non-pairwise comparisons (*$P \le 0.05$; **$P \le 0.01$; ***$P \le 0.001$). We calculated fold change value from the ratio of EC_{50} (NE +PAGln) to EC_{50} (PAGln), SEM (standard error of the mean) value was calculated from the 14 mean EC_{50} values generated by analyzing each individual human muscle data separately and the p-value was calculated using two-tailed unpaired Welch's t-test by comparing the mean EC_{50} values for individual replicates between the groups (NE+PAGln and PAGln). Data was obtained from 14 muscles ($n = 9$ human subjects, NE+ PAGln) and from 9 muscles ($n = 6$ human subjects, NE). All reported P values are two-sided. A P-value of <0.05 was considered significant in this study.

NAM activity (see below). For example, docking studies suggested that when PAGln is docked to AS1, it putatively interacts with residue E122 of the transmembrane helical domain 3, residue T164 of the transmembrane helical domain 4, and residues V206 and S207 of the transmembrane helical domain 5 (Fig. 6). Candidate amino acid residues involved in PAGln interaction at additional candidate sites that were functionally tested are also illustrated in Fig. 6 (expanded views).

The results of functional interrogation of mutagenesis studies of the AS1 site of β2AR in the presence vs absence of PAGln are shown in Fig. 7. HTLA cells transfected with either WT or single-site mutant *ADRB2*-Tango plasmid constructs were examined for ISO-induced cAMP dose-response (left column panels) and β-arrestin2 recruitment assays (right column panels). The synthetic negative allosteric modulator AS408 was used as positive control for NAM activity (Figs. S14A and S14B). Mutagenesis of residues E122, V206, and T164 produced a β2AR that retained functional activity like WT with respect to both cAMP production (cAMP normalized Figures: 7A, 7C, 7E and 7G; cAMP absolute value Figures: S14F, S14G, S14H and S14I) and β-arrestin2 recruitment (Figs. 7B, 7D, 7F, 7H, S14B, S14C, S15B, S15C, S15D and S15E). Moreover, both E122L and V206M mutants demonstrated substantial attenuation in PAGln induced NAM activity (Fig. 7C–F). Specifically, we found that while the E122L-β2-Tango and V206M-β2-Tango mutants retained the normal ISO-treated cAMP and β-arrestin2 recruitment dose-responses, the NAM effect of PAGln observed with WT β2AR was completely abolished with both mutants using both cAMP and β-arrestin2 recruitment functional assays (Fig. 7). These data indicate that mutations E122L and V206M in the AS1 pocket of β2AR are critical in propagating PAGln induced NAM activity. In contrast, the

allosteric activity of PAGln remained unaffected with the T164V-β2-Tango mutant (another predicted residue within the AS1 site), suggesting T164 is not critical for the NAM β2AR activity of PAGln (i.e., PAGln still showed NAM activity for both ISO-induced cAMP dose-response (Fig. 7G) and β-arrestin2 recruitment (Figs. 7H and S15D).

Discussion

The human gut microbiome produces a vast array of metabolites that act as signaling molecules and substrates for metabolic reactions within the host[41–43]. Our studies indicate that PAGln, a gut microbe-generated metabolite recently shown to be both clinically and mechanistically linked to CVD[8] and heart failure[9,10], functions as a negative allosteric modulator (NAM) of β2AR, but not β1AR. As far as we are aware, the present studies are the first report of a gut microbe-generated metabolite that functions as a negative allosteric modulator of a host GPCR. Historically, drug discovery efforts targeting GPCRs have focused on agonists and antagonists that bind to the orthosteric site of the receptor. But the pursuit of allosteric modulators has become important in recent years, as they have the potential to fine-tune cellular responses with greater selectivity among the subtypes of GPCRs in tissues where the endogenous agonist exerts its physiological effect[23,24]. In this regard, synthetic allosteric modulators, which specifically act as pharmacological agents, have expanded the understanding of the downstream signaling mediated by GPCRs[22,44,45]. In the present studies, PAGln in isolation transiently functioned as a partial agonist of β2AR, yet under chronic exposure to PAGln (as exists in vivo) and in the presence of agonists, such as under sympathetic tone as exists in vivo, PAGln diminishes functional responses of β2-agonists
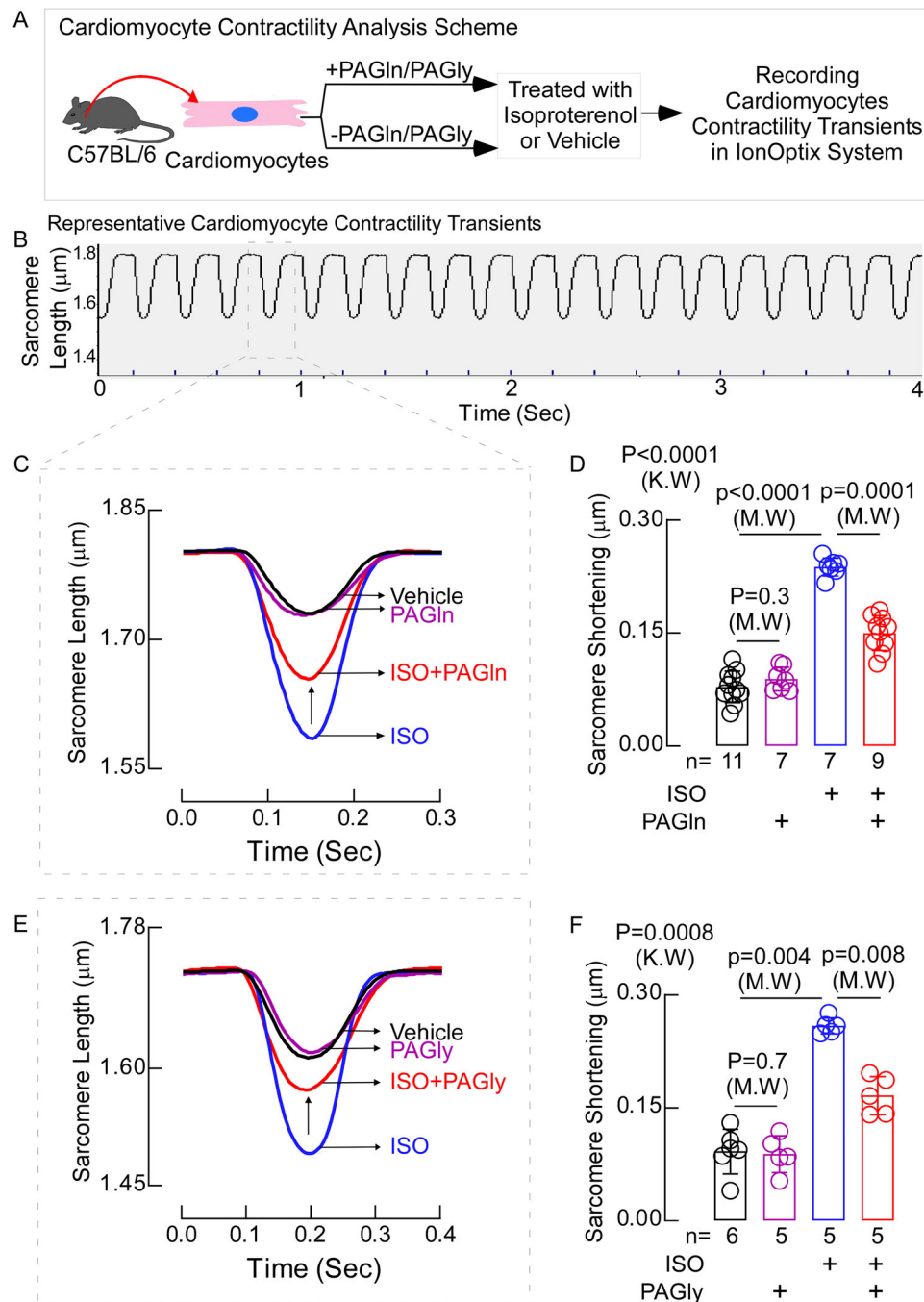
Fig. 5 | Effect of PAGln and PAGly on ISO-induced mouse cardiomyocyte contractility. A Experimental design of mouse ventricular cardiomyocyte contractility assay. Ventricular cardiomyocytes were isolated from adult C57BL/6 mice and contractility was measured using an IonOptix System under various conditions as indicated. **B** Representative cardiomyocyte contractility trace displaying changes in sarcomere length over time. **C** Cardiomyocyte contractility trace of ventricular cardiomyocytes from WT C57BL/6 mice after treating them with 10 μM ISO (Blue), 10 μM ISO with 100 μM PAGln (Red), 100 μM PAGln alone (Purple), or vehicle control (Black). **D** Quantification of the sarcomere shortening of each cardiomyocytes form (**C**) expressed as bar graph. **E** Contractility trace of ventricular cardiomyocyte

from WT C57BL/6 mice after treatment with 10 μM ISO (Blue), 10 μM ISO with 100 μM PAGly (Red), 100 μM PAGly alone (Purple), and vehicle control (Black). **F** Quantification of sarcomere shortening of each cardiomyocytes form (**E**) expressed as bar graph. Data points represent the mean ± SD (n = cardiomyocytes from at least 3 mice). The nonparametric two-tailed Mann–Whitney test was used for non-pairwise comparisons and the two-sided Kruskal–Wallis test with Dunn's post hoc test was performed for multiple comparisons in (**D**) ($P < 0.0001$) and (**F**) ($P = 0.0008$). All reported P values are two-sided. A P-value of <0.05 was considered significant in this study (*$P \leq 0.05$; **$P \leq 0.01$; ***$P \leq 0.001$).

both in isolated cardiomyocytes and in failing human heart ventricular tissue explants. This constellation of behaviors from an allosteric ligand represents a relatively emerging and less-explored class of allosteric modulators, referred to as ago-allosteric modulators, meaning they display both agonism on their own and allosteric effects when co-incubated with their respective agonist[46]. It is worth noting

that the partial agonist activity of PAGln was only observed transiently during acute exposure (i.e., with PAGln incubations of ~8 min it is observed (Fig. S1A), yet with longer incubations no effect with PAGln alone were observed). Under physiological conditions involving chronic exposure to PAGln in the presence of endogenous β-agonist, PAGln functions as a negative allosteric modulator (i.e., with PAGln
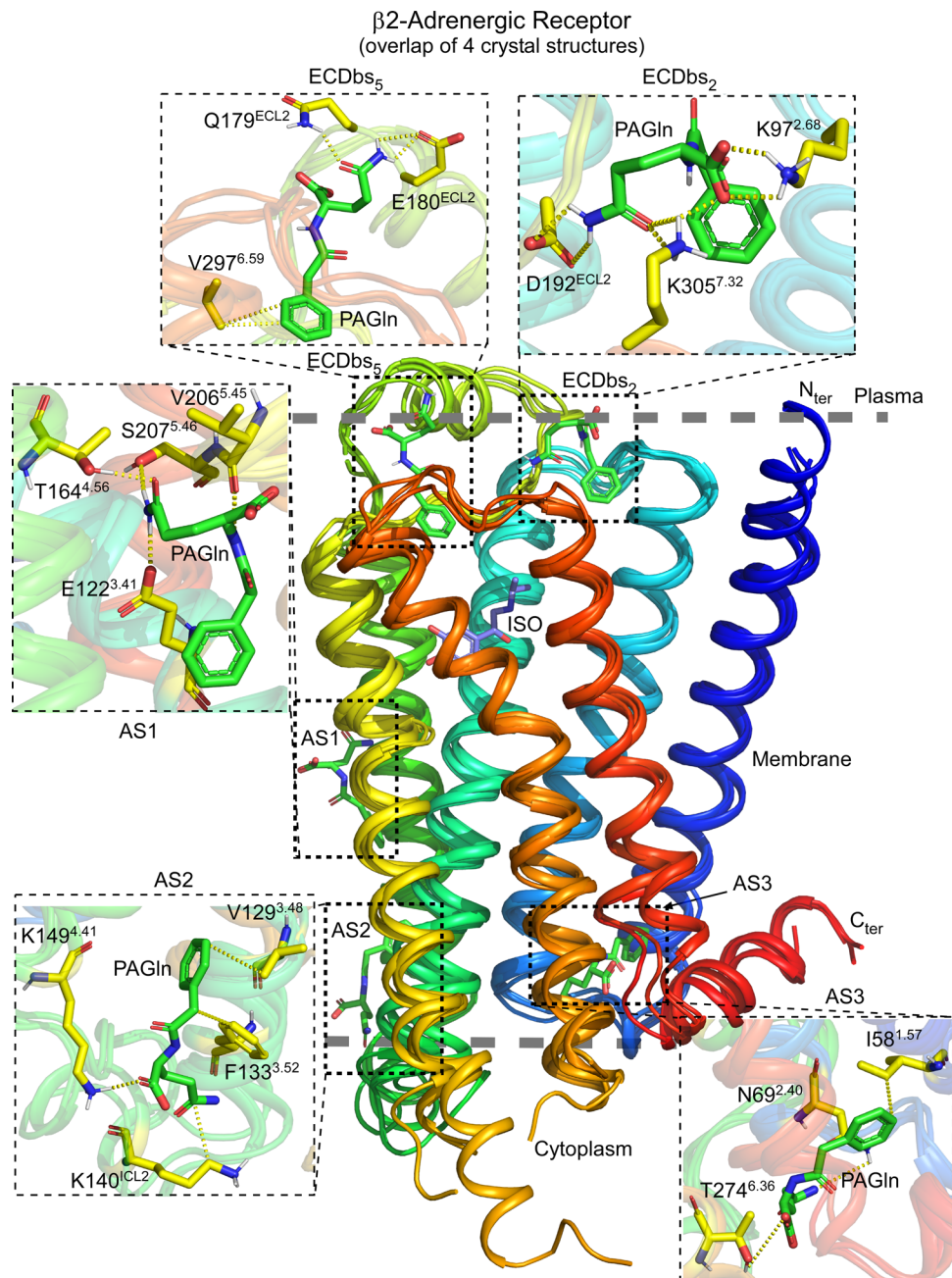
Fig. 6 | PAGln docking to extracellular candidate binding sites and to known allosteric sites of β2AR. Superimposed crystal structures of β2AR depicting iso-proterenol (ISO, purple) bound to the orthosteric site of β2AR (PDB id: 7DHR) is used to illustrate the interaction of PAGln with amino acids from candidate/allosteric binding sites of β2AR selected for further mutagenesis studies. The top section shows PAGln docked to two extracellular candidate binding sites (ECDbs$_2$ and ECDbs$_5$, dashed boxes) found by PAGln unbiased docking, that bind PAGln relatively strong (ΔG_{bind} = −5.99 and −5.07 kcal/mol, Table S2). The interaction of PAGln with amino acid residues in close proximity is shown in expanded views for each

site. The middle and bottom sections show PAGln bound to three known allosteric sites (dashed boxes): allosteric site 1 (AS1, for NAM AS408, PDB id: 6OBA), allosteric site 2 (AS2, for PAM Cmpd-6FA, PDB id: 6N48), and allosteric site 3 (AS3, for NAM Cmpd-15PA, PDB id: 5X7D). The expansion views show the interaction of docked PAGln with amino acids in close proximity. Amino acid residues selected for further site-directed mutagenesis studies (Table S5) are within 5 Å of the docked PAGln in each of the five binding sites shown here. The mutated residues are: K97 and K305 (ECDbs$_2$); Q179 and E180 (ECDbs$_5$); E122, T164, V206, and S207 (AS1); F133, K149 (AS2); and N69, T274 (AS3).

incubations of ≥25 min as in Fig. S1C, how virtually all studies were performed except where indicated). Furthermore, given that PAGln's partial agonistic behavior is observed exclusively in cAMP generation and not in β-arrestin2 recruitment, it is appropriate to characterize PAGln as a negative allosteric modulator (NAM) with biased partial agonism.

Based on our results using human myocardial tissues, murine cardiomyocytes, and genetically engineered cell systems, PAGln functions as a NAM, diminishing responses triggered by orthosteric

β2AR ligands. Our biochemical data show that large molar excesses of PAGln fail to directly compete for [3H]-propranolol binding (Fig. 3B), consistent with a PAGln interaction site on β2AR distinct from the orthosteric site. Site-directed mutagenesis and functional studies of residues E122 and V206 of β2AR (Fig. 6, Table S5) suggest that mutations of these residues (E122L, V206M) modulate the NAM effect of PAGln. Despite being distant in the primary sequence, residues E122 and V206 are in close spatial proximity in the intact receptor, and this region of β2AR appears critical for propagating PAGln-induced NAM
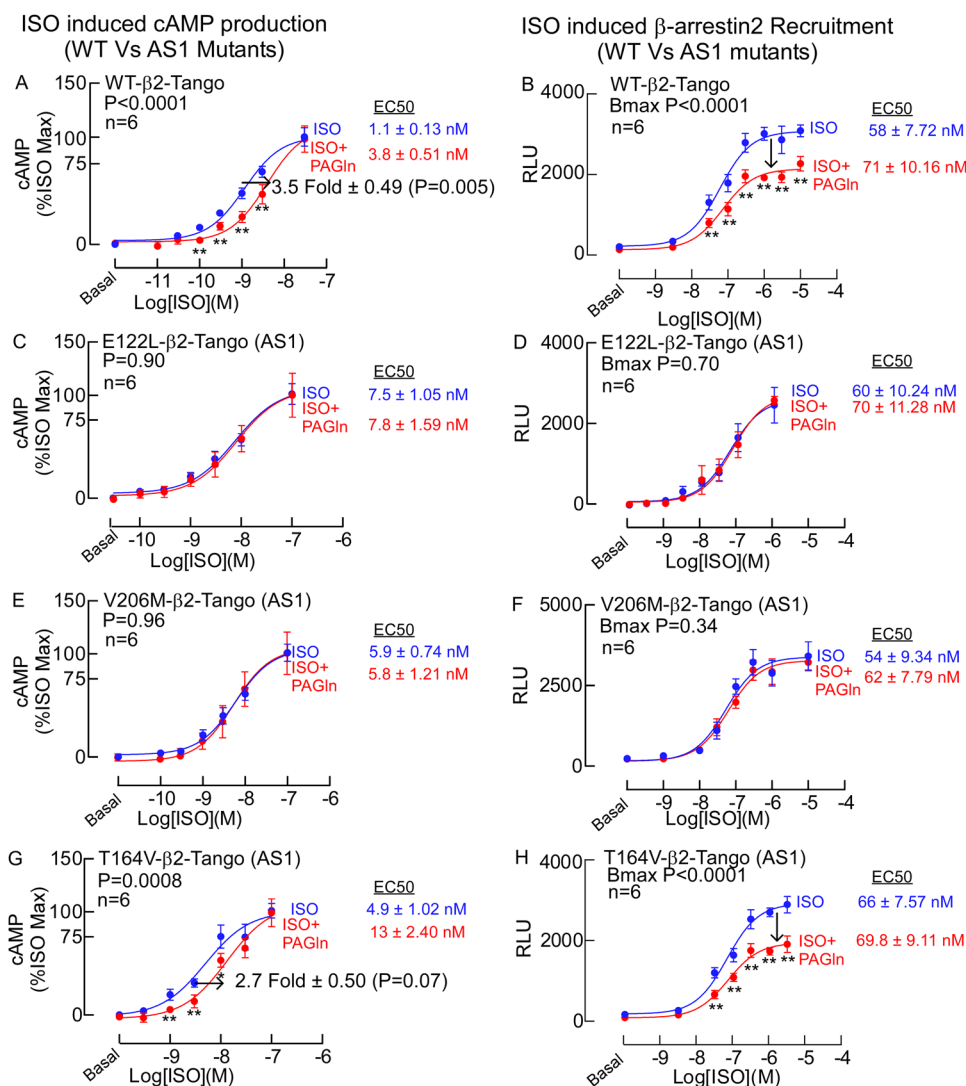
Fig. 7 | PAGln effect on ISO-induced cAMP dose-response and β-arrestin2 recruitment in WT and mutant β2ARs in HTLA cells. A–H cAMP dose-response (left) and β-arrestin2 recruitment (right) in HLTA cells with increasing doses of ISO alone (Blue) or ISO with 100 μM PAGln (Red), after transfecting them with WT β2AR (**A, B**), E122L β2AR (**C, D**), V206M β2AR (**E, F**), and T164V β2AR (**G, H**) Tango plasmid constructs. Maximum cAMP response is normalized to 100% and basal response to zero. β-arrestin2 recruitment was measured as relative luminance unit (RLU). $EC_{50} \pm SEM$ of the cAMP dose-responses and B_{max} of β-arrestin2 recruitment dose response in each panel are shown as indicated. P values at the top left for cAMP graphs compare EC_{50} values (Blue vs Red). P values at the top left for β-arrestin2 recruitment graphs compare B_{max} values (Blue vs Red). Data points represent the mean ± SD of the indicated number (n) of experiments. P value (top left) for B_{max} comparisons (Blue vs Red) as well as the EC_{50}s and the standard error of the mean EC_{50} (SEM) were determined with a non-linear regression method. In (**A**) and (**G**), two-tailed unpaired Welch's student t-tests were used to obtain the fold change P-values when comparing the EC_{50} values for ISO and ISO+PAGln from three different experiments (ISO vs ISO+PAGln for (**A**), P = 0.005; ISO vs ISO+PAGln for (**G**), P = 0.07). Nonparametric two-tailed Mann–Whitney test was used for non-pairwise comparisons (*P ≤ 0.05; **P ≤ 0.01; ***P ≤ 0.001). All reported P values are two-sided. A P-value of <0.05 was considered significant in this study.

activity in β2AR. It is notable that crystallography studies using the synthetic allosteric modulator AS408 previously showed AS408 binds to this site, and suggested this region functions as a conformational hub, impacting transition between a higher versus lower affinity state[27]. More recent studies examining the contribution of these residues as determinants of ligand efficiency and potency in GPCR signaling has further identified mutations at these sites as passenger mutations[47].

While targeted docking points to several amino acid residues of β2AR (namely E122, T164, V206, S207) that were predicted to interact with PAGln (when the docking was restricted to the binding pocket of AS408, PDB id: 6OBA), the actual binding site of PAGln on β2AR and the mechanism by which PAGln exhibits its NAM effect remain unknown. We note that AS1 (AS408 binding pocket based on co-crystallography studies[27]) is located on the surface of β2AR at a site

predicted to be buried within the membrane. While the synthetic allosteric ligand AS408 (volume of 284 Å[3]) is similar in size to PAGln (267 Å[3]), AS408 has significant hydrophobic character (e.g., cLogP of 3.72) compared to the highly polar PAGln (cLogP of −1.27; Fig. S16). Thus, while the physicochemical properties of AS408 might allow it to penetrate the membrane and bind to this region on β2AR, it is difficult to imagine PAGln could do the same due to its hydrophilicity. Yet studies with intact membranes from β2AR transfected cells clearly reveal that PAGln induces a NAM effect on β2AR signaling. Furthermore, the NAM activity of PAGln was also observed within both intact cardiomyocytes and strips of human failing myocardial (ventricular) tissue. Until crystallography studies confirm whether PAGln interacts directly at this site, we think it is appropriate to emphasize that the present data merely shows these residues are essential for propagating the NAM effect of PAGln. We also note that the other synthetic

allosteric modulators reported−Cmpd-6FA (co-crystalized at AS2[28]) and Cmpd-15PA (co-crystalized at AS3[24])−are almost three times as large as PAGln (674 Å^3 and 749 Å^3, respectively, Fig. S16), and considerably more hydrophobic (cLogP: 4.41 and 5.1, respectively, Fig. S16). In this context, our mutagenesis studies led to surprising results. We were not able to experimentally confirm any of the putative binding sites predicted by in silico approaches, but rather, only found that mutating amino acid residues E122 and V206 (within the AS408 binding pocket−a previously reported "conformational hub" [25]), abolished PAGln's NAM effect. Importantly, in our studies, mutation of E122 or V206 showed no significant effect on canonical orthosteric ligand-driven β2AR functions (both cAMP and β-arrestin2).

Another notable finding in the present studies is that PAGln not only attenuates β2AR function but also displays receptor subtype selectivity, a characteristic feature of allosteric modulators. PAGln has greater affinity for β2AR compared to β1AR. We thus speculate that the striking clinical associations noted between circulating PAGln levels and adverse pathophysiological outcomes[8,9], along with the effects of PAGln-mediated in vivo thrombosis that have been shown in animal model studies to be attenuated by the presence of β-blockers[8], are likely attributable (at least in part) to the β2AR-selective NAM effects of PAGln observed in the present studies. β1AR is present in excess to β2AR in both the healthy human heart and during heart failure. However, during heart failure, the relative proportion of β2AR significantly increases, suggesting an enhanced role of β2AR in progressive heart failure[38–40]. Changes in β2AR-induced cAMP signaling have also been suggested to contribute to adverse clinical outcomes and impaired exercise capacity in subjects with heart failure[40,48]. In the present studies, exposure to high levels of PAGln (but well within levels observed in multiple different clinical cohorts[8,30,34,49]) were shown to reduce cardiomyocyte contractility and isometric LV heart muscle contraction (Figs. 4 and 5).

Certain limitations to our studies should be acknowledged. The present studies explored in detail the NAM functional activity observed with PAGln in β2AR, as opposed to β1AR. However, our previous studies with platelets demonstrated PAGln can signal through alternative ARs (e.g., α2A and α2B in platelets; ref. 8). Whether PAGln manifests NAM behavior with these or other ARs remains to be determined. Additionally, though at least 2 residues critical for transmitting the NAM effect of PAGln in β2AR have been identified, the exact binding site on β2AR remains to be unambiguously established. Further, while use of beta blocking agents has become a mainstay of heart failure pharmacotherapy, the impact of inhibiting the NAM effect induced by PAGln in vivo remains to be established.

The present studies raise exciting possibilities for modulation of AR signaling by altering gut microbial PAGln production and suggest that therapeutic targeting of the PAGln pathway merits further investigation. It is remarkable to think that co-evolution of *Homo sapiens* with our microbial symbionts resulted in the development of host-sensing mechanisms of microbial metabolites that fine tune host GPCRs. PAGln is a product of metaorganismal metabolism, produced by the concerted action of gut microbiota on dietary protein phenylalanine, and host hepatic conjugation of the microbial metabolite following absorption into the portal circulation. Such co-evolution suggests that PAGln production may confer physiological benefit under certain conditions. Notably, we recently showed that PAGln elicits B-type natriuretic peptide gene expression in both cultured cardiomyoblasts and murine atrial tissue[9], an activity that could theoretically promote a beneficial adaptive response to congestion during heart failure. Further exploration of the metaorganismal PAGln pathway, along with its involvement in physiological processes and disease states where adrenergic receptors (especially β2AR) are known to play a role, represent future topics of research. More broadly, the role of gut microbiota-generated metabolites in regulating host GPCR signaling is an exciting and promising area for future investigation.

Methods

Cell culture
Cell culture experiments were performed utilizing the following cell lines: HEK293 (ATCC Cat#CRL-1573), β2-HEK293 (stable line generated in this study), β1-HEK293 (stable line generated in this study), and HTLA cells (gift from the Bryan Roth Laboratory). All HEK293 cell lines were cultured in DMEM supplemented with 10% fetal bovine serum (FBS), 100 U/mL penicillin, and 100 μg/mL streptomycin, and maintained in a humidified atmosphere at 37 °C with 5% CO_2. Cells were seeded into 96-well plates at a density of ~50,000 cells per well and subjected to various experimental treatments following incubation in a specific stimulation buffer. HTLA cells, derived from HEK293 cells and engineered to stably express a tTA-dependent luciferase reporter and a β-arrestin2-TEV fusion gene, were maintained in DMEM supplemented with 10% FBS, 100 U/mL penicillin, 100 μg/mL streptomycin, 2 μg/mL puromycin, and 100 μg/mL hygromycin B. Transfections were performed using Lipofectamine 3000, with ~85% efficiency, to introduce WT or mutant ADRB2-Tango plasmids. The cell culture protocols ensured consistent growth and preparation for subsequent assays, including cAMP measurements, β-arrestin2 recruitment, and radioligand binding.

cAMP dose-response in β1-HEK293, β2-HEK293, parental-HEK293, and HTLA cells
Intracellular cAMP dose-responses were measured using CatchPoint Cyclic-AMP Fluorescent Assay Kit from molecular devices (Cat. R8089)[8]. β1-HEK293, β2-HEK293, parental-HEK293 and transiently transfected HTLA cells, re-suspended in 100 μL stimulation buffer (1X HBSS, 20 mM HEPES pH 7.4, 0.5 mM IBMX, 0.1 mM Rolipram and 0.1% BSA) were treated with increasing concentrations of the test compounds (isoproterenol, norepinephrine, phenylalanine and PAGln) for 8 min in a 37 °C incubator. To analyze PAGln's allosteric behavior, the cells were incubated with 100 μM of PAGln for 15 min at room temperature, followed by addition of increasing concentration of β-agonists (isoproterenol and norepinephrine), and kept for 10 min in a 37 °C incubator. Thereafter, the reaction was stopped by adding 50 μL of lysis buffer, followed by cAMP levels in the lysed samples were quantified following manufactures recommendation. All cAMP data were normalized, with the minimum response set to zero and the maximum response set to 100%. For detailed experimental procedures, please refer to the Supplementary Methods file.

β-Arrestin2 recruitment assay in HTLA cells
β-arrestin2 recruitment was performed on HTLA cells provided by the laboratory of Dr. Bryan L Roth[36]. Briefly, HTLA cells were transfected with a WT *ADRB2*-Tango plasmid (Roth Lab PRESTO-Tango GPCR Kit-Addgene #Cat 1000000068) or mutant *ADRB2*-Tango plasmids (E122L, E122Q, V206M, T164V, S207C, and S207N) using the Lipofactamine 3000 transfection kit (Invitrogen, Cat #L3000008). After 48 h of transfection, 100 μM of PAGln in assay buffer (20 mM HEPES and 1X HBSS, pH 7.4) were added (10 μL of 10X concentration) to the respective wells of the 96-well plate. Following incubation with PAGln for 90 min, increasing concentration of β-agonists (isoproterenol or norepinephrine) were added (25 μL of 5X concentration) as indicated. The following day, the plate content was aspirated, and 100 μL of Bright-Glo solution (Promega, #Cat E2620) diluted 5-fold in the assay buffer was added to each well and after 10 min luminescence was measured as relative luminescence units (RLU). For detailed experimental procedures, please refer to the Supplementary Methods file.

Membrane preparation and radioligand binding assay
β2-HEK293 (and parental control cell) membranes were prepared for the radioligand binding studies[8]. For saturation binding, 10 μg of the β2-HEK293 membranes were pre-incubated with 100 μM PAGln or 10 mM ISO at 15 °C for 15 min in binding buffer (75 mM Tris-HCl (pH

7.4), 12.5 mM $MgCl_2$ and 2 mM EDTA). Next, increasing concentration of [^{3}H]-propranolol (23.3 Ci/mmol; 43 μM, Perkin Elmer, Waltham, MA) were added into the reaction mixture as indicated. For competition radioligand binding, unbound radioisotopes were washed and 10 μg of the membranes in binding buffer (75 mM Tris·HCl (pH 7.4), 12.5 mM $MgCl_2$ and 2 mM EDTA) were incubated with 100 μM of PAGln for 15 min, then different concentrations of ISO were added to the reaction mixture as indicated. Next, 1 nmole of [^{3}H]-propranolol (23.3 Ci/mmol; 43 pmoles/μL, Perkin Elmer, Waltham, MA) was added and incubated for 1 h at 15 °C water bath. For both saturation and competition binding assays membranes were harvested and washed, and radioactivity was measured using a Liquid Scintillation Counter (Beckman, LSC6000sc, Indianapolis, IN). As a further control, for studies we confirmed that [^{3}H]-propranolol shows specific binding only to β2-HEK293 cell membranes and not to the parental control cell membranes. For detailed experimental procedures, please refer to the Supplementary Methods file.

Dynamic mass redistribution (DMR) studies on β2-HEK293 cells
The DMR experiments were performed on β2-HEK293 stable cell line[8]. Briefly, the cells were grown in EPIC-corning fibronectin-coated 96-well DMR microplates (Cat. 5082-Corning) for one day before the DMR experiment. The following day, cells were washed with 1X HBSS buffer with HEPES (20 mM, pH 7.4), and basal DMR responses were monitored using a Corning Epic BT system (Corning Epic-product code 5053) for 15 min to obtain a baseline reading. Thereafter, different concentrations of isoproterenol were added as indicated, and the DMR signal (in picometer) was monitored for 60 min. For allosteric modulator studies, PAGln (final concentration 100 μM) was incubated in the respective wells for 30 min before adding isoproterenol. For detailed experimental procedures, please refer to the Supplementary Methods file.

Human heart tissue procurement and cardiac muscle function
All participants gave written informed consent (IRB 2378 approved by Cleveland Clinic, Ohio). Left ventricular apical tissue was removed from patients with heart failure undergoing left ventricular assist device (LVAD) insertion surgery at the Cleveland Clinic, Ohio. Trabecular muscles were dissected to measure isometric contractility[50–52]. Briefly, muscles from each heart were randomly separated into two groups: PAGln-treated or non-PAGln treated control. After 15 min pretreatment with 100 μM PAGln (PAGln-treated group only), a norepinephrine dose-response curve (NE, range: 1 nM to 100 μM) was obtained from all muscles from both groups. NE curves were normalized to the response obtained at the highest dose (100 μM NE). For detailed experimental procedures, please refer to the Supplementary Methods file.

Isolation of mouse cardiomyocytes and contractility studies
All procedures were approved by the Institutional Animal Care and Use Committee (IACUC), ensuring compliance with ethical standards for animal handling, welfare monitoring, and euthanasia. Male C57BL/6J mice, 12–14 weeks old, were purchased from The Jackson Laboratory and maintained in our facilities. Mice were kept under a 14-h light/10-h dark cycle, with food and water available ad libitum, at 20–26 °C and 30–70% humidity. For cardiomyocyte isolation, mice were anesthetized, and hearts were excised, cannulated with a 20-gauge needle, and mounted onto a Langendorff perfusion apparatus. Hearts were perfused for 4 min with a buffer containing 113 mM NaCl, 4.7 mM KCl, 0.6 mM KH_2PO_4, 0.6 mM Na_2HPO_4, 1.2 mM $MgSO_4$, 0.5 mM $MgCl_2$, 10 mM HEPES, 20 mM D-glucose, 30 mM taurine, and 20 μM Ca^{2+} at pH 7.4, maintained at 34 °C with continuous oxygenation (95% O_2, 5% CO_2). Subsequently, 150 units/mL of type II collagenase were perfused for 15 min. Left ventricular tissue was isolated, minced, and digested for 15 min. The digested tissue was filtered through 200 μm mesh,

centrifuged to isolate viable myocytes. For contractility studies, myocytes underwent serial washes, Ca^{2+} concentration was increased to 1.8 mM, and contractility was assessed using an IonOptix System (Myopace, Milton, MA)[53,54]. Isolated myocytes were plated on glass chamber slides and placed on the microscope stage (Leica) connected to a field stimulator specifically designed for driving isolated myocytes (MyoPace, IonOptix). Cardiomyocyte contractility transients were measured as sarcomere length (μm) and sarcomere shortening (μm). Myocytes were treated with 10 μM of isoproterenol and cardiomyocytes contractility transients were recorded. For allosteric studies, the myocytes were pre-incubated with either 100 μM PAGln or PAGly for 15 min before addition of isoproterenol. For detailed experimental procedures, please refer to the Supplementary Methods file.

Site-directed mutagenesis
Site-directed mutagenesis to replace individual amino acids (E122L, E122Q, T164V, V206M, S207C, and S207N) of *ADRB2*-Tango plasmid was performed by PCR using the QuickChange II Site-Directed Mutagenesis kit (Agilent). Briefly, 10 ng of the *ADRB2*-Tango plasmid was amplified with PfuUltra HF DNA Polymerase (Agilent) and each of the desired mutant encoding paired DNA oligos, and the PCR products were digested with Dpn1 and transformed into Stellar chemically competent cells (Takara). The cells were then plated on LB-Ampicillin plates and incubated overnight at 37 °C. Individual bacterial colonies were picked and grown overnight, and plasmids were isolated. We sequenced the plasmids with a primer using the sequence upstream of the mutation sites (ggcgcagctcatatcctga) to confirm the desired mutation. AS2, AS3, ECDbs$_2$, and ECDbs$_5$ mutants were synthesized by Genscript (Piscataway, NJ) based on the *ADRB2*-Tango DNA sequence. Details of the primers used is described in Supplemental Methods.

In silico approach for the detection of PAGln candidate binding sites in β2AR
To identify potential binding sites for PAGln in β2AR, we first performed an untargeted search using the program AutoLigand[55] to identify candidate binding sites in β2AR for molecules of PAGln's size by using the following four crystal structures of the receptor: PDB ids: 6OBA, 5X7D, 6N48, and 7DHR. In the second step, PAGln was unbiased docked to the 4 crystal structures of β2AR with the docking program AutoDock4[56]. The PAGln candidate binding sites identified are listed in Table S2. Four PAGln candidate binding sites (2 extracellular: ECDbs$_2$, ECDbs$_5$, and 2 intracellular: ICDbs$_1$, ICDbs$_2$) discussed here are shown in Figs. S5 and S7. To get a better estimation of the predicted binding affinity of PAGln to candidate binding sites mapped out through PAGln unbiased docking to β2AR, we refined the docking by allowing the side chain of residues in the candidate binding site to rotate freely around single bonds. Finally, we refined the docking for PAGln bound to the 2 extracellular and 2 intracellular candidate binding sites identified using PAGln unbiased docking (shown in Fig. S9). The predicted binding free energy of PAGln to these sites and a list of the residues within 5 Å of PAGln in the candidate binding site are provided in Table S3. In the last step of the in silico approach, we performed targeted docking of PAGln to the orthosteric and known allosteric sites of β2AR (PDB ids: 7DHR, 5X7D, 6OBA, and 6N48[26–28]) using the Schrodinger software package (Schrodinger, LLC, NY, USA)[57]. The induced fit docking (IFD) protocol (Schrodinger, LLC, NY, USA)[58] was further used to allow for flexibility of the side chain residues in the active site, and to improve the binding affinities by re-docking the ligands. The binding affinity was estimated by the Glide XP program through the XP GlideScore[59]. The IFD protocol uses a combination of the XP GlideScore and the energy calculated by the Prime program (XP GlideScore + 0.05 × PrimeEnergy) to take into account the reorganization energy of the protein active site and the ligand, and to rank the final set of protein-ligand complexes. The detailed procedure for the in silico approach to identifying

candidate binding sites in β2AR and putative amino acid residues that modulate PAGln's NAM activity is described in the Supplement.

Statistics

The normality distribution of the data was determined using the Shapiro−Wilk test. For non-pairwise comparisons, the nonparametric two-tailed Mann−Whitney U test for non-parametric data and the parametric two-tailed Welch's student t-test for parametric data were used. For multiple comparisons (three or more groups), the two-sided Kruskal−Wallis test with Dunn's post hoc test was employed for non-parametric data, and the two-way ANOVA with Bonferroni's post-tests was used for parametric data. GraphPad PRISM 10.0 was used to create graphs and statistics. Each dose-response (DR) curve includes duplicate data points for each experiment, and each experimental DR study is repeated with at least three replicates, with the findings indicating full best-fit DR curves to the cumulative data. The EC_{50} values were determined by fitting curves to the whole DR dataset. Each replicate value was treated as a separate point in the analysis. P-values were generated to compare the EC_{50} values of two distinct fitted curves in graphs displaying the EC_{50} curves. The fold-change values were calculated from the ratio of EC_{50} (with PAGln) to EC_{50} (without PAGln), SEM (standard error of the mean) values were derived from the three mean EC_{50} values obtained from each individual replicate experiment, and fold change P-values were calculated by comparing the means of the EC_{50}s generated from each dose-response curve across three different replicate experiments. The data distribution was assessed using Prism's Shapiro−Wilk normality test. Furthermore, P-values were determined using two-tailed unpaired Welch's student t-test (for parametric data) and two-tailed Mann−Whitney U-test (for non-parametric data) to compare the mean EC_{50}s between the groups (with and without PAGln). All reported P values are two-sided. A P-value of <0.05 was considered significant in this study. There were no statistical approaches used to predict the sample sizes. No data were excluded from the analysis. DR analyses were performed in GraphPad PRISM 10.0 using the non-linear regression method. Non-linear regressions were fitted with the equation "log(inhibitor) vs response − three parameters". All DRC analyses were fitted with the least squares regression method. B_{max} and K_d values were determined using Prism's site-specific binding equations.

Data availability

Source data is made available in the public data sharing repository Zenodo (https://doi.org/10.5281/zenodo.10568333). Any additional information required to reanalyze the data reported in this paper is available from the lead contact upon request. The protein structures can be found at The Worldwide Protein Data Bank (wwPDB), accompanied by their respective links: 7DHR, 6OBA, 6N48, 5X7D. Source data are provided with this paper.

References

1. Sartor, R. B. & Wu, G. D. Roles for intestinal bacteria, viruses, and fungi in pathogenesis of inflammatory Bowel diseases and therapeutic approaches. *Gastroenterology* **152**, 327–339.e324 (2017).
2. Ahmed, S. & Spence, J. D. Sex differences in the intestinal microbiome: interactions with risk factors for atherosclerosis and cardiovascular disease. *Biol. Sex. Differ.* **12**, 35 (2021).
3. Gilbert, J. A. et al. Current understanding of the human microbiome. *Nat. Med.* **24**, 392–400 (2018).
4. Pluznick, J. L. The gut microbiota in kidney disease. *Science* **369**, 1426–1427 (2020).
5. Zwartjes, M. S. Z., Gerdes, V. E. A. & Nieuwdorp, M. The role of gut microbiota and its produced metabolites in obesity, dyslipidemia, adipocyte dysfunction, and its interventions. *Metabolites* **11**, 531 (2021).
6. Koh, A. & Backhed, F. From association to causality: the role of the gut microbiota and its functional products on host metabolism. *Mol. Cell* **78**, 584–596 (2020).
7. Witkowski, M., Weeks, T. L. & Hazen, S. L. Gut microbiota and cardiovascular disease. *Circ. Res.* **127**, 553–570 (2020).
8. Nemet, I. et al. A cardiovascular disease-linked gut microbial metabolite acts via adrenergic receptors. *Cell* **180**, 862–877.e822 (2020).
9. Romano, K. A. et al. Gut microbiota-generated phenylacetylglutamine and heart failure. *Circulation: Heart Fail.* **16**, e009972 (2022).
10. Tang, W. H. W. et al. Prognostic value of gut microbe-generated metabolite phenylacetylglutamine in patients with heart failure. *Eur. J. Heart Fail* **26**, 233–241 (2024).
11. Liu, Y. et al. Phenylacetylglutamine is associated with the degree of coronary atherosclerotic severity assessed by coronary computed tomographic angiography in patients with suspected coronary artery disease. *Atherosclerosis* **333**, 75–82 (2021).
12. Fang, C. et al. Dysbiosis of gut microbiota and metabolite phenylacetylglutamine in coronary artery disease patients with stent stenosis. *Front. Cardiovasc. Med.* **9**, 832092 (2022).
13. Zhu, Y. et al. Two distinct gut microbial pathways contribute to meta-organismal production of phenylacetylglutamine with links to cardiovascular disease. *Cell Host Microbe* **31**, 18–32.e19 (2023).
14. Wang, J., Gareri, C. & Rockman, H. A. G-Protein-coupled receptors in heart disease. *Circ. Res.* **123**, 716–735 (2018).
15. Lymperopoulos, A., Cora, N., Maning, J., Brill, A. R. & Sizova, A. Signaling and function of cardiac autonomic nervous system receptors: Insights from the GPCR signalling universe. *FEBS J.* **288**, 2645–2659 (2021).
16. Ciccarelli, M., Santulli, G., Pascale, V., Trimarco, B. & Iaccarino, G. Adrenergic receptors and metabolism: role in development of cardiovascular disease. *Front. Physiol.* **4**, 265 (2013).
17. Hein, L. & Kobilka, B. K. Adrenergic receptors from molecular structure to in vivo function. *Trends Cardiovasc. Med.* **7**, 137–145 (1997).
18. Graham, R. M. Adrenergic receptors: structure and function. *Cleve Clin. J. Med.* **57**, 481–491 (1990).
19. Reid, J. L. Alpha-adrenergic receptors and blood pressure control. *Am. J. Cardiol.* **57**, 6E–12E (1986).
20. Madamanchi, A. Beta-adrenergic receptor signaling in cardiac function and heart failure. *McGill J. Med.* **10**, 99–104 (2007).
21. Wold, E. A. & Zhou, J. GPCR allosteric modulators: mechanistic advantages and therapeutic applications. *Curr. Top. Med. Chem.* **18**, 2002–2006 (2018).
22. Wootten, D., Christopoulos, A. & Sexton, P. M. Emerging paradigms in GPCR allostery: implications for drug discovery. *Nat. Rev. Drug Discov.* **12**, 630–644 (2013).
23. Weis, W. I. & Kobilka, B. K. The molecular basis of G protein-coupled receptor activation. *Annu. Rev. Biochem.* **87**, 897–919 (2018).
24. Wisler, J. W., Rockman, H. A. & Lefkowitz, R. J. Biased G protein-coupled receptor signaling: changing the paradigm of drug discovery. *Circulation* **137**, 2315–2317 (2018).
25. Ahn, S. et al. Small-molecule positive allosteric modulators of the beta2-adrenoceptor isolated from DNA-encoded libraries. *Mol. Pharm.* **94**, 850–861 (2018).
26. Liu, X. et al. Mechanism of intracellular allosteric beta2AR antagonist revealed by X-ray crystal structure. *Nature* **548**, 480–484 (2017).
27. Liu, X. et al. An allosteric modulator binds to a conformational hub in the beta2 adrenergic receptor. *Nat. Chem. Biol.* **16**, 749–755 (2020).
28. Liu, X. et al. Mechanism of beta2AR regulation by an intracellular positive allosteric modulator. *Science* **364**, 1283–1287 (2019).

29. Thal, D. M., Glukhova, A., Sexton, P. M. & Christopoulos, A. Structural insights into G-protein-coupled receptor allostery. *Nature* **559**, 45–53 (2018).

30. Zong, X. et al. Phenylacetylglutamine as a risk factor and prognostic indicator of heart failure. *ESC Heart Fail* **9**, 2645–2653 (2022).

31. McDonagh, T. A. et al. 2023 Focused Update of the 2021 ESC Guidelines for the diagnosis and treatment of acute and chronic heart failure. *Eur. Heart J.* **44**, 3627–3639 (2023).

32. Heidenreich, P. A. et al. 2022 AHA/ACC/HFSA guideline for the management of heart failure: executive summary: a report of the American College of Cardiology/American Heart Association Joint Committee on Clinical Practice Guidelines. *J. Am. Coll. Cardiol.* **79**, 1757–1780 (2022).

33. Meyer, T. W. et al. Kt/Vurea and nonurea small solute levels in the hemodialysis study. *J. Am. Soc. Nephrol.* **27**, 3469–3478 (2016).

34. Poesen, R. et al. Microbiota-derived phenylacetylglutamine associates with overall mortality and cardiovascular disease in patients with CKD. *J. Am. Soc. Nephrol.* **27**, 3479–3487 (2016).

35. Sirich, T. L., Funk, B. A., Plummer, N. S., Hostetter, T. H. & Meyer, T. W. Prominent accumulation in hemodialysis patients of solutes normally cleared by tubular secretion. *J. Am. Soc. Nephrol.* **25**, 615–622 (2014).

36. Kroeze, W. K. et al. PRESTO-Tango as an open-source resource for interrogation of the druggable human GPCRome. *Nat. Struct. Mol. Biol.* **22**, 362–369 (2015).

37. Schroder, R. et al. Applying label-free dynamic mass redistribution technology to frame signaling of G protein-coupled receptors noninvasively in living cells. *Nat. Protoc.* **6**, 1748–1760 (2011).

38. Woo, A. Y. & Xiao, R. P. beta-Adrenergic receptor subtype signaling in heart: from bench to bedside. *Acta Pharm. Sin.* **33**, 335–341 (2012).

39. Bristow, M. R. et al. Beta 1- and beta 2-adrenergic-receptor subpopulations in nonfailing and failing human ventricular myocardium: coupling of both receptor subtypes to muscle contraction and selective beta 1-receptor down-regulation in heart failure. *Circ. Res.* **59**, 297–309 (1986).

40. Nikolaev, V. O. et al. Beta2-adrenergic receptor redistribution in heart failure changes cAMP compartmentation. *Science* **327**, 1653–1657 (2010).

41. Krautkramer, K. A., Fan, J. & Backhed, F. Gut microbial metabolites as multi-kingdom intermediates. *Nat. Rev. Microbiol.* **19**, 77–94 (2021).

42. Tang, W. H. W., Li, D. Y. & Hazen, S. L. Dietary metabolism, the gut microbiome, and heart failure. *Nat. Rev. Cardiol.* **16**, 137–154 (2019).

43. Brown, J. M. & Hazen, S. L. The gut microbial endocrine organ: bacterially derived signals driving cardiometabolic diseases. *Annu. Rev. Med.* **66**, 343–359 (2015).

44. Christopoulos, A., May, L. T., Avlani, V. A. & Sexton, P. M. G-protein-coupled receptor allosterism: the promise and the problem(s). *Biochem. Soc. Trans.* **32**, 873–877 (2004).

45. May, L. T., Leach, K., Sexton, P. M. & Christopoulos, A. Allosteric modulation of G protein-coupled receptors. *Annu. Rev. Pharm. Toxicol.* **47**, 1–51 (2007).

46. Schwartz, T. W. & Holst, B. Allosteric enhancers, allosteric agonists and ago-allosteric modulators: where do they bind and how do they act? *Trends Pharm. Sci.* **28**, 366–373 (2007).

47. Heydenreich, F. M. et al. Molecular determinants of ligand efficacy and potency in GPCR signaling. *Science* **382**, eadh1859 (2023).

48. Wagoner, L. E. et al. Polymorphisms of the beta(2)-adrenergic receptor determine exercise capacity in patients with heart failure. *Circ. Res.* **86**, 834–840 (2000).

49. Ottosson, F. et al. The gut microbiota-related metabolite phenylacetylglutamine associates with increased risk of incident coronary artery disease. *J. Hypertens.* **38**, 2427–2434 (2020).

50. Dhillon, A. et al. Association of noninvasively measured left ventricular mechanics with in vitro muscle contractile performance: a prospective study in hypertrophic cardiomyopathy patients. *J. Am. Heart Assoc.* **3**, e001269 (2014).

51. Bennett, M. K. et al. S100A1 in human heart failure: lack of recovery following left ventricular assist device support. *Circ. Heart Fail* **7**, 612–618 (2014).

52. Ogletree, M. L. et al. Duration of left ventricular assist device support: effects on abnormal calcium cycling and functional recovery in the failing human heart. *J. Heart Lung Transpl.* **29**, 554–561 (2010).

53. Li, D., Wu, J., Bai, Y., Zhao, X. & Liu, L. Isolation and culture of adult mouse cardiomyocytes for cell signaling and in vitro cardiac hypertrophy. *J. Vis. Exp* **87**, 51357 (2014).

54. Vasudevan, N. T., Mohan, M. L., Gupta, M. K., Hussain, A. K. & Naga Prasad, S. V. Inhibition of protein phosphatase 2A activity by PI3K-gamma regulates beta-adrenergic receptor function. *Mol. Cell* **41**, 636–648 (2011).

55. Harris, R., Olson, A. J. & Goodsell, D. S. Automated prediction of ligand-binding sites in proteins. *Proteins* **70**, 1506–1517 (2008).

56. Morris, G. M. et al. AutoDock4 and AutoDockTools4: automated docking with selective receptor flexibility. *J. Comput. Chem.* **30**, 2785–2791 (2009).

57. Jacobson, M. P. et al. A hierarchical approach to all-atom protein loop prediction. *Proteins* **55**, 351–367 (2004).

58. Sherman, W., Day, T., Jacobson, M. P., Friesner, R. A. & Farid, R. Novel procedure for modeling ligand/receptor induced fit effects. *J. Med. Chem.* **49**, 534–553 (2006).

59. Friesner, R. A. et al. Extra precision glide: docking and scoring incorporating a model of hydrophobic enclosure for protein-ligand complexes. *J. Med. Chem.* **49**, 6177–6196 (2006).

Acknowledgements

Author contributions

P.P.S. participated in the design, performance, and analysis of most studies. P.P.S. and V.G. contributed to the drafting of the manuscript with input from all authors. M.L.M. and J.A. assisted in the radioligand binding studies. V.G. and K.D.S. performed the in silico docking studies. W.S. participated in the human heart muscle contraction analysis. N.K. assisted in site-directed mutagenesis studies. C.W. and K.S. assisted in mouse cardiomyocyte contractility studies. D.M. assisted with statistical analysis. T.A. provided scientific input in contractility studies. J.A. participated in synthesizing AS408. V.G., S.S.K., S.V.N.P., C.S.M., M.A.F., J.M.B., and J.A.D. provided critical scientific input and took part in thoughtful discussions. S.L.H. conceived, designed, and supervised all studies and the drafting and editing of the manuscript. All authors contributed to the critical review of the manuscript.

Competing interests

Additional information

Supplementary information The online version contains supplementary material available at https://doi.org/10.1038/s41467-024-50855-3.

Correspondence and requests for materials should be addressed to Stanley L. Hazen.

Peer review information *Nature Communications* thanks the anonymous reviewers for their contribution to the peer review of this work. A peer review file is available.

Reprints and permissions information is available at http://www.nature.com/reprints

Publisher's note Springer Nature remains neutral with regard to jurisdictional claims in published maps and institutional affiliations.